



Radiative b-hadron decays at LHCb

Yingrui Hou (LPCA, CNRS)
On behalf of the LHCb collaboration

22nd Conference on Flavor Physics and CP Violation (FPCP 2024)
Chulalongkorn University, 27th-31st May 2024

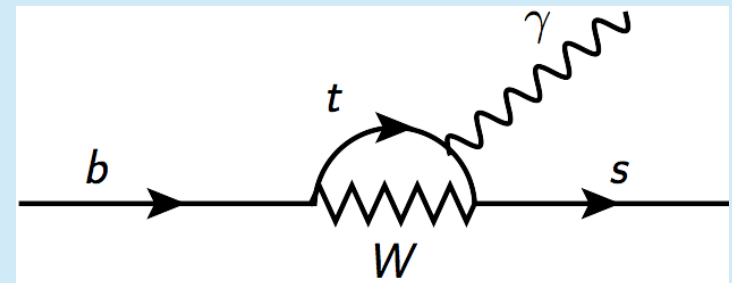
Radiative b-hadron decays

- On the theory side

- FCNC is strongly suppressed by the Standard Model (SM)
- Sensitive to indirect effects of New Physics (NP)
- Access to test couplings to 3rd generation quarks

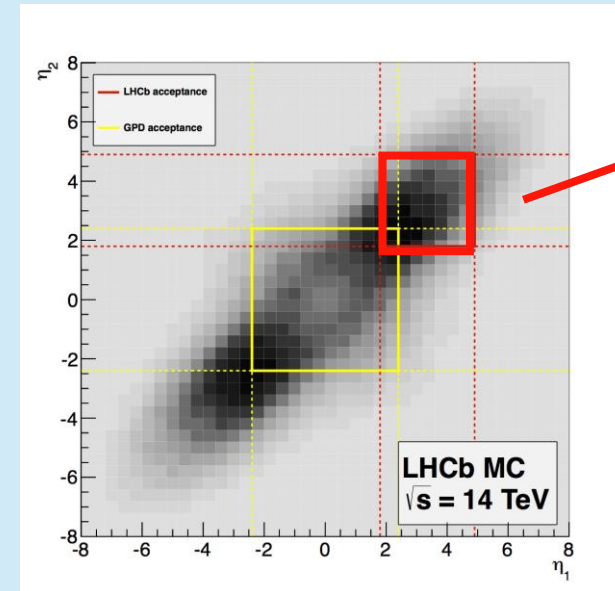
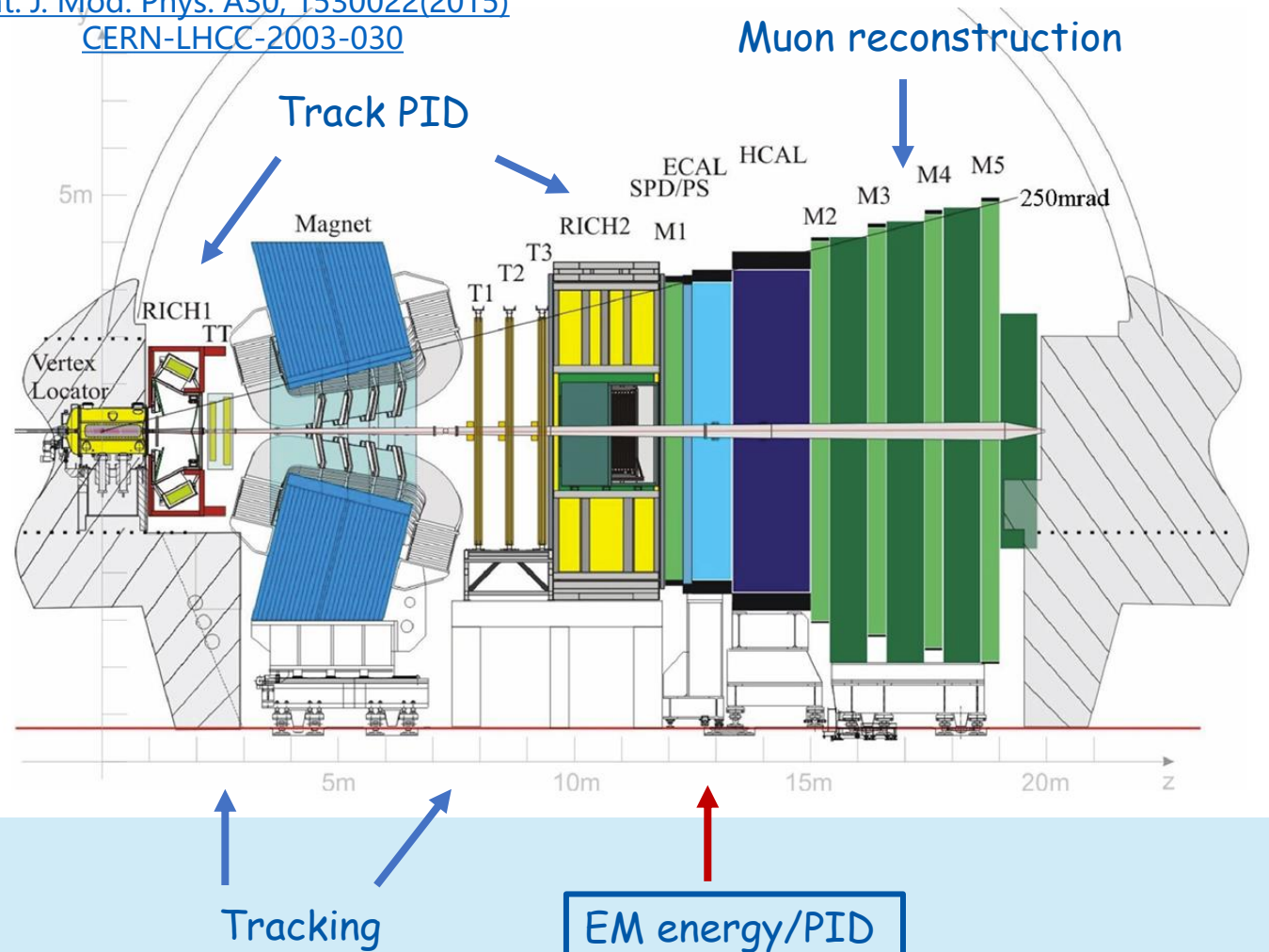
- On the measurement side

- Search for the unobserved decays
 - > *measurement of branching fraction/upper limit*
- Amplitude study for the multibody decays
 - > *hadron spectrum at photon pole*
 - > *photon polarisation*



LHCb: A flavour physics detector with high luminosity

[Int. J. Mod. Phys. A30, 1530022\(2015\)](#)
[CERN-LHCC-2003-030](#)



LHCb:
27% of b or \bar{b}
 $* \sigma_{b\bar{b}} = 72 \mu\text{b}$ (7 TeV)
 $= 154 \mu\text{b}$ (13 TeV)

[*PRL118\(2017\)052002](#)

- Forward spectrometer, focusing on $b\bar{b}$ production
- Performance
 - $\epsilon_{\text{tracking}} \sim 96\%$
 - ECAL resolution: $1\% + \frac{10\%}{\sqrt{E(\text{GeV})}}$

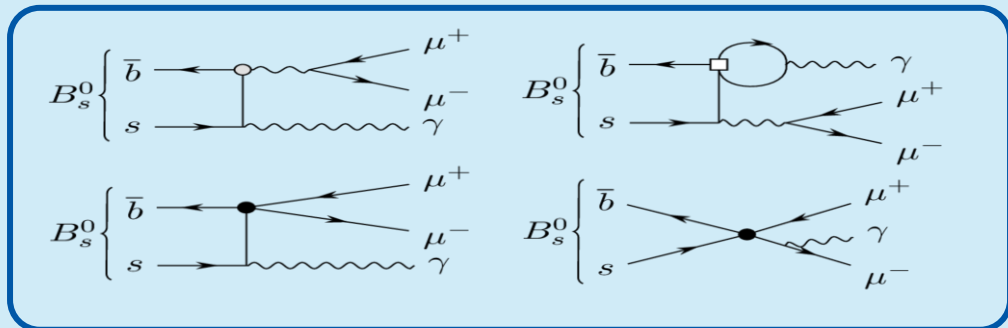
Searching for the unobserved decays

$B_s^0 \rightarrow \mu^+ \mu^- \gamma$: [arxiv.2404.03375](https://arxiv.org/abs/2404.03375)

Searching for $B_s^0 \rightarrow \mu^+ \mu^- \gamma$ decay

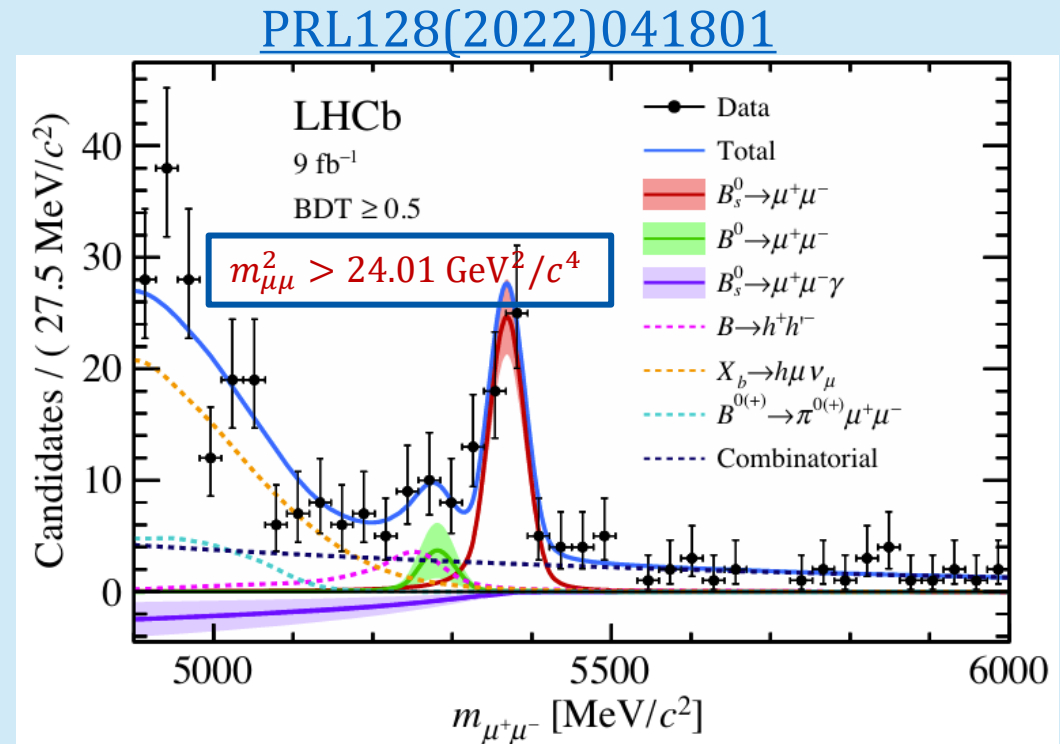
[arxiv.2404.03375](https://arxiv.org/abs/2404.03375)

- $B_s^0 \rightarrow \mu^+ \mu^- \gamma$ vs. $B_s^0 \rightarrow \mu^+ \mu^-$
 - ☺ Sensitive to a different set of Wilson coefficients: (C_7, C_9, C_{10}) vs (C_S, C_P, C_{10})
 - ☺ The photon lifts the helicity suppression making $Br(B_s^0 \rightarrow \mu^+ \mu^-) \sim Br(B_s^0 \rightarrow \mu^+ \mu^- \gamma)$
 - ☹ Larger theoretical uncertainties $\rightarrow B_s^0 \rightarrow \gamma$ form factor
 - ☹ Worse mass resolution due to the photon reconstruction



Theory prediction [[JHEP 11\(2017\) 184](https://doi.org/10.1088/1126-6708/2017/11/184)]

- $q^2 < 8.64 \text{ GeV}^2/c^4$:
 $Br(B_s^0 \rightarrow \mu^+ \mu^- \gamma) = (8.3 \pm 1.3) \times 10^{-9}$
- $q^2 > 15.84 \text{ GeV}^2/c^4$:
 $Br(B_s^0 \rightarrow \mu^+ \mu^- \gamma) = (8.9 \pm 1.0) \times 10^{-9}$

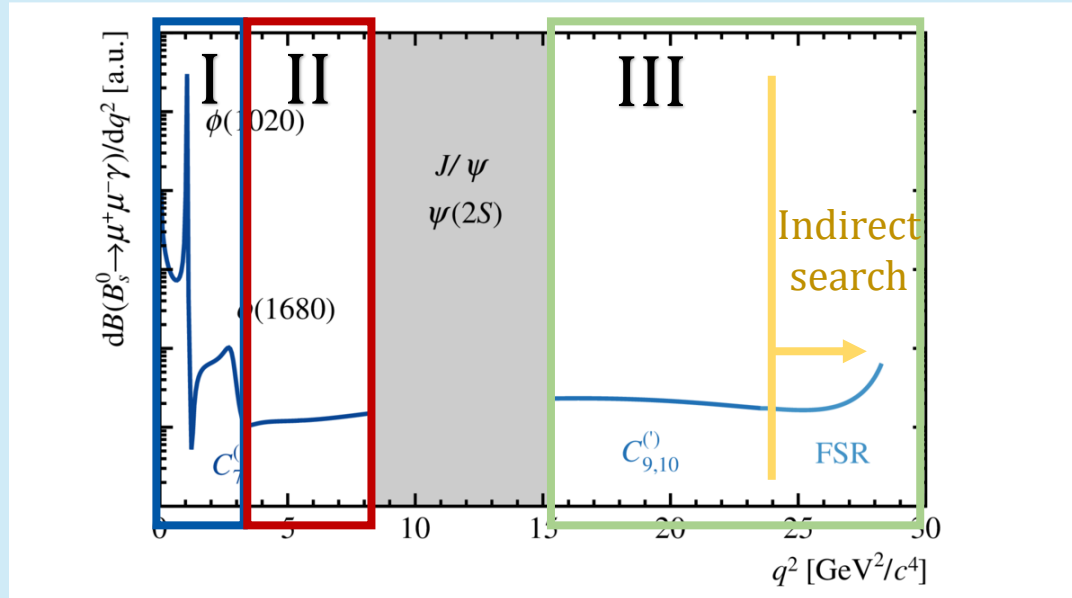


Searching for $B_s^0 \rightarrow \mu^+\mu^-\gamma$ decay

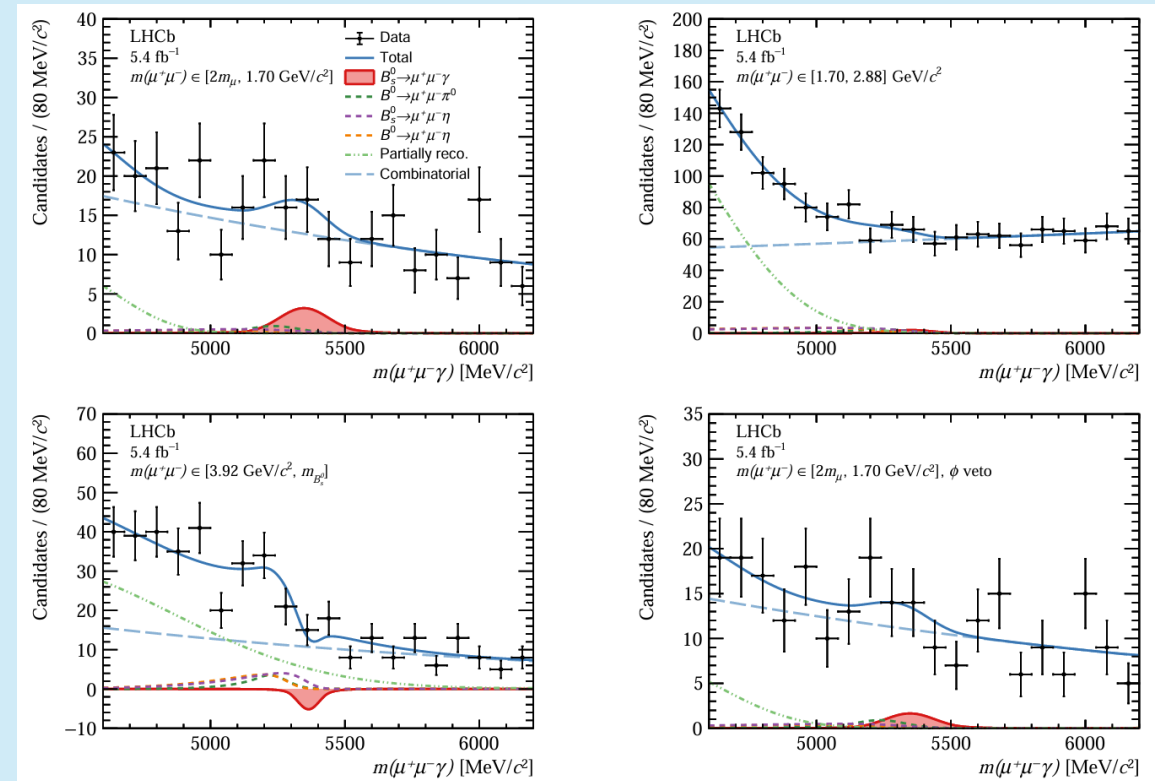
[arxiv.2404.03375](https://arxiv.org/abs/2404.03375)

- Strategy

- 2016-2018 data (5.4fb^{-1})
- Searching in 3 q^2 regions (ϕ -vetoed bin I is also studied)
- Control channel: $B_s^0 \rightarrow \phi(KK)\gamma$
 - Check the agreement between data and simulation
- Normalisation channel: $B_s^0 \rightarrow J/\psi(\mu\mu)\eta(\gamma\gamma)$
 - High statistics + Similar final state to the signal



Mass fit of $B_s^0 \rightarrow \mu\mu\gamma$ in all q^2 regions



Searching for $B_s^0 \rightarrow \mu^+ \mu^- \gamma$ decay

[arxiv.2404.03375](https://arxiv.org/abs/2404.03375)

• Results

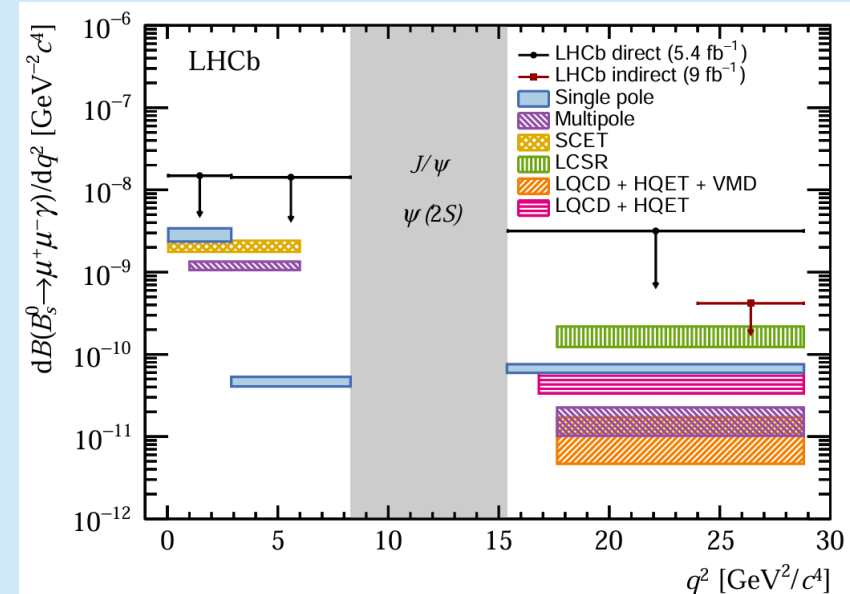
- First direct search of $B_s^0 \rightarrow \mu\mu\gamma$ at low q^2
- No statistically significant signal is observed in all q^2 regions

• Constrain in the theoretical context

- Indirect method reaches lower ULs
- Direct search is more sensitive to the full q^2 spectrum
 - New constraints in the low q^2 region

• Run3 data will improve the sensitivity of the search

$$\begin{aligned}\mathcal{B}(B_s^0 \rightarrow \mu^+ \mu^- \gamma)_I &< 3.6(4.2) \times 10^{-8}, \\ \mathcal{B}(B_s^0 \rightarrow \mu^+ \mu^- \gamma)_{II} &< 6.5(7.7) \times 10^{-8}, \\ \mathcal{B}(B_s^0 \rightarrow \mu^+ \mu^- \gamma)_{III} &< 3.4(4.2) \times 10^{-8}, \\ \mathcal{B}(B_s^0 \rightarrow \mu^+ \mu^- \gamma)_I, \text{ with } \phi \text{ veto} &< 2.9(3.4) \times 10^{-8}, \\ \mathcal{B}(B_s^0 \rightarrow \mu^+ \mu^- \gamma)_{\text{comb.}} &< 2.5(2.8) \times 10^{-8},\end{aligned}$$



Amplitude analyses of the multibody decays

$\Lambda_b \rightarrow p K^- \gamma$: [arxiv.2403.03710](https://arxiv.org/abs/2403.03710)

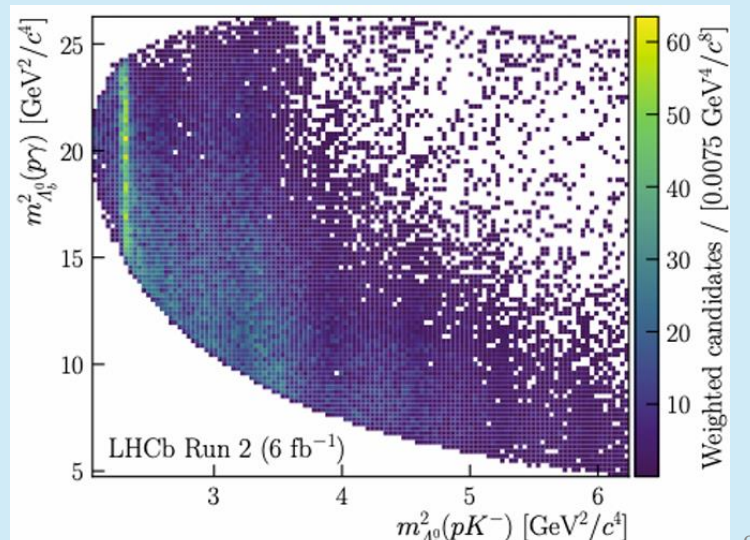
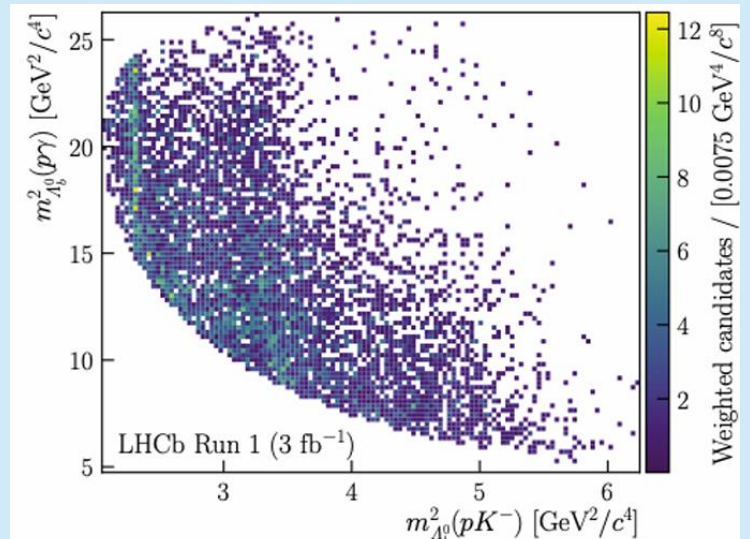
$B_s^0 \rightarrow K K \gamma$: LHCb-paper-2024-002 (in preparation)

Amplitude analysis of $\Lambda_b \rightarrow p K^- \gamma$

[arxiv.2403.03710](https://arxiv.org/abs/2403.03710)

- The $\Lambda_b \rightarrow p K \gamma$ provides information about the composition of the $p K^-$ spectrum with unique access to the heavier Λ states.
 - Could constitute useful input to future measurements of photon polarization in $b \rightarrow s \gamma$
 - Vital input to low energy-QCD (light baryon) theory
- Strategy
 - Using full Run1 and Run2 data
 - Building amplitude model with helicity formalism
 - Performing unbinned maximum likelihood fit to the Dalitz plane ($m_{pK}^2, m_{p\gamma}^2$)

$$\begin{aligned}
 & \text{connect } p \text{ and } \Lambda^* \text{ helicity frames} \\
 & d_{\lambda_p \lambda_\Lambda}^{J_\Lambda}(\theta_p) \times \sum_{L=|J_{\Lambda_b^0}-S|}^{|J_{\Lambda_b^0}+S|} \sum_{S=|J_\Lambda-J_\gamma|}^{|J_\Lambda+J_\gamma|} \left[\begin{array}{c} C_1 C_2 C_3 \quad \text{Clebsch-Gordans} \\ \text{Wigner d} \end{array} \right. \\
 & \quad \left. \begin{array}{c} \text{fit parameter} \\ h_{LS}^\Lambda \\ \text{LS coupling} \end{array} \right] \left(\frac{p}{M_{\Lambda_b^0}} \right)^L \left(\frac{q}{M_\Lambda} \right)^I B_L(p) B_I(q) \text{BW}_I(m_{pK}) \\
 & \quad \text{line shape with form factors} \\
 & \quad \text{orb. ang. mom. barriers}
 \end{aligned}$$

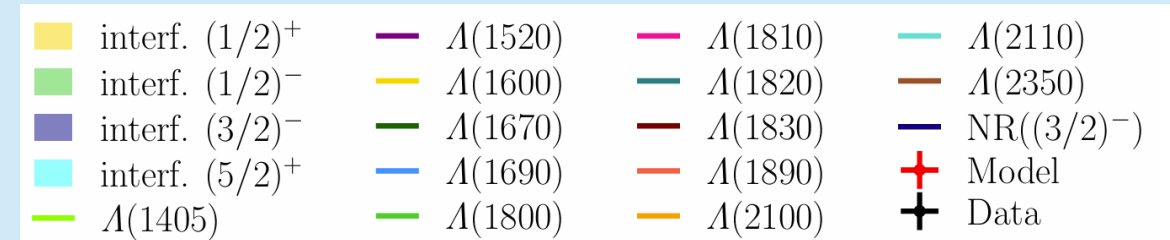
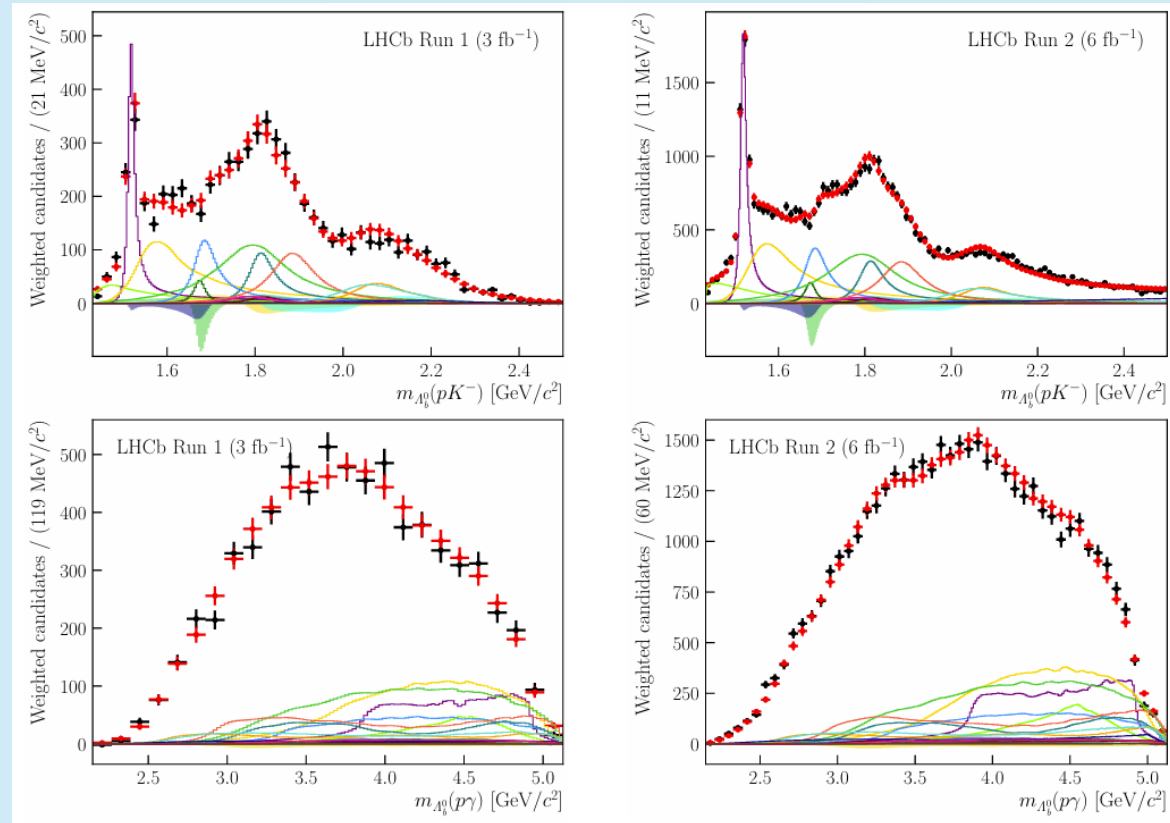


Amplitude analysis of $\Lambda_b \rightarrow pK^-\gamma$

arxiv.2403.03710

- The default fit model

- All known Λ states + a nonresonant contribution ($J^P = \frac{3}{2}^-$)



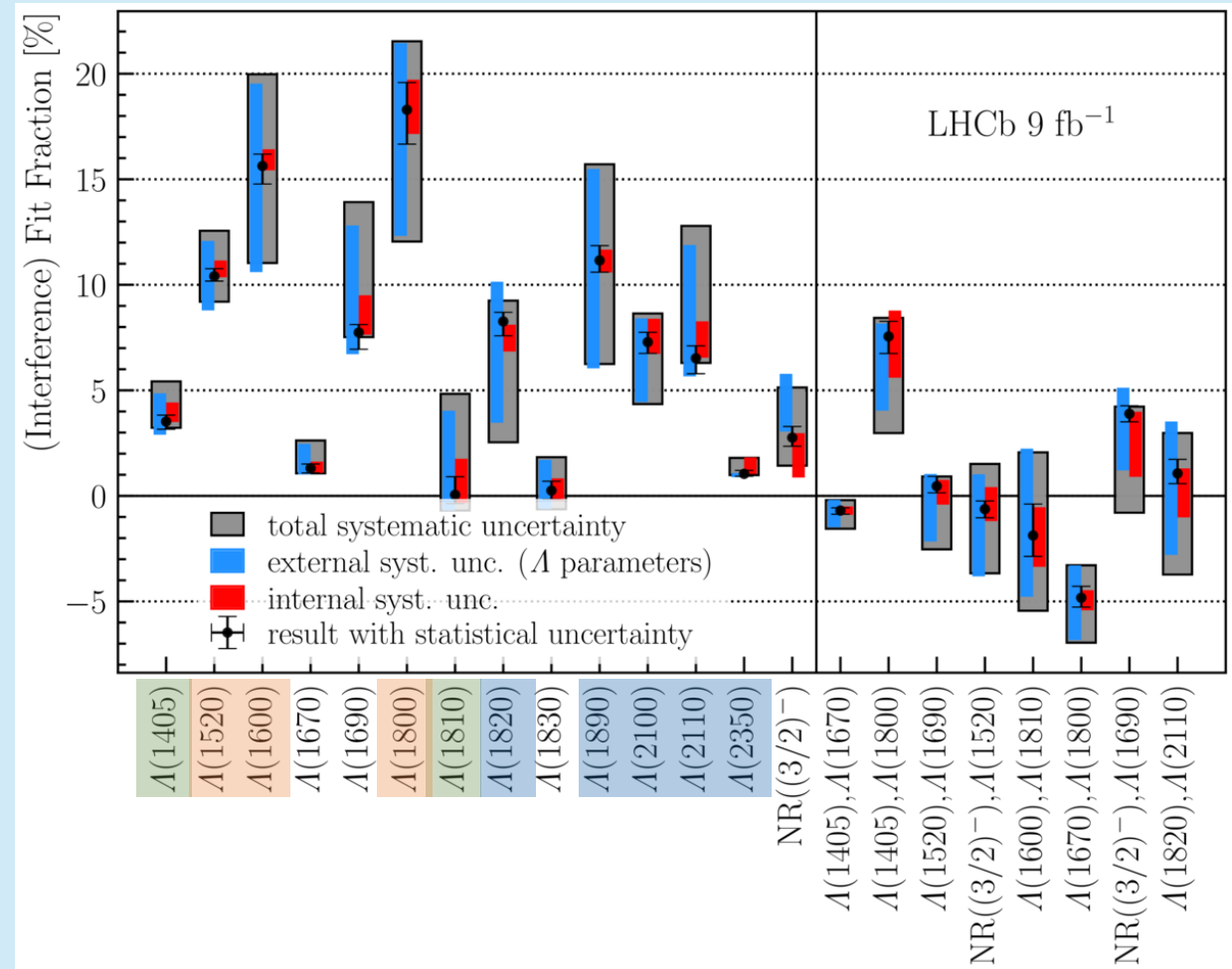
- The uncertainties

- Resonance parameters (external input)
 - Dominant uncertainty
- Statistics
- Model-related systematic uncertainties
 - Model choice and mass resolution
- Other uncertainties
 - Mass fit, acceptance model, background estimation

Amplitude analysis of $\Lambda_b \rightarrow pK^-\gamma$

arxiv.2403.03710

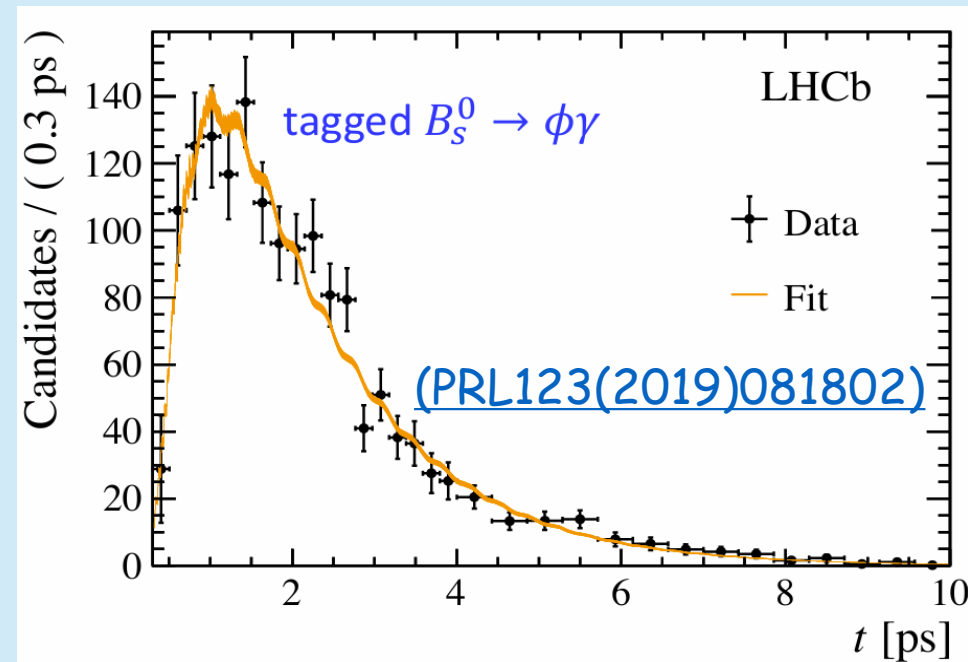
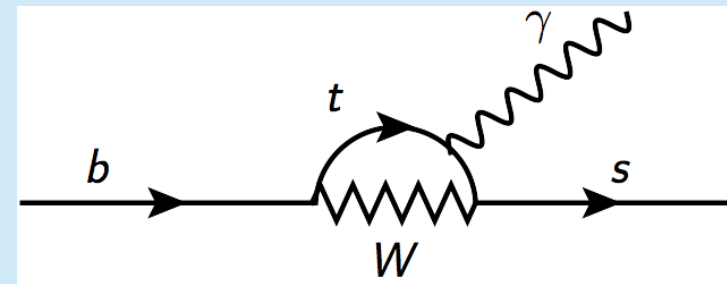
- Results are given in terms of fit and interference fractions
- The largest resonant contributions are $\Lambda(1800)$, $\Lambda(1600)$, $\Lambda(1890)$ and $\Lambda(1520)$
- Compared to $\Lambda_b \rightarrow J/\psi pK$
 - Contributions of $\Lambda(1405)$, $\Lambda(1810)$ are smaller, while contribution of $\Lambda(1820)$ is larger
 - Heavy resonances $\Lambda(1890)$, $\Lambda(2100)$, $\Lambda(2110)$ and $\Lambda(2350)$ are larger in the radiative case
- Future measurements and data will improve the precision



Amplitude analysis of $B_s^0 \rightarrow KK\gamma$

LHCb-paper-2024-002

- One of the golden channels of $b \rightarrow s\gamma$ transition
 - Dominated by a virtual intermediate top quark coupled to a W boson
 - Photon polarisation in $B_s^0 \rightarrow \phi\gamma$ has been measured by LHCb
 - $\sim 1.5 - 2\sigma$ compatibility with the SM
 - Possible new radiative decay modes with KK resonance?
- Strategy
 - Full Run1 and Run2 data
 - Building amplitude with isobar model in the folded helicity semi-plane (m_{KK} , $|\cos \theta_{KK}|$)
 - Decay rate asymmetry of B_s is neglected
 - Mass resolution is included



Amplitude analysis of $B_s^0 \rightarrow KK\gamma$

LHCb-paper-2024-002

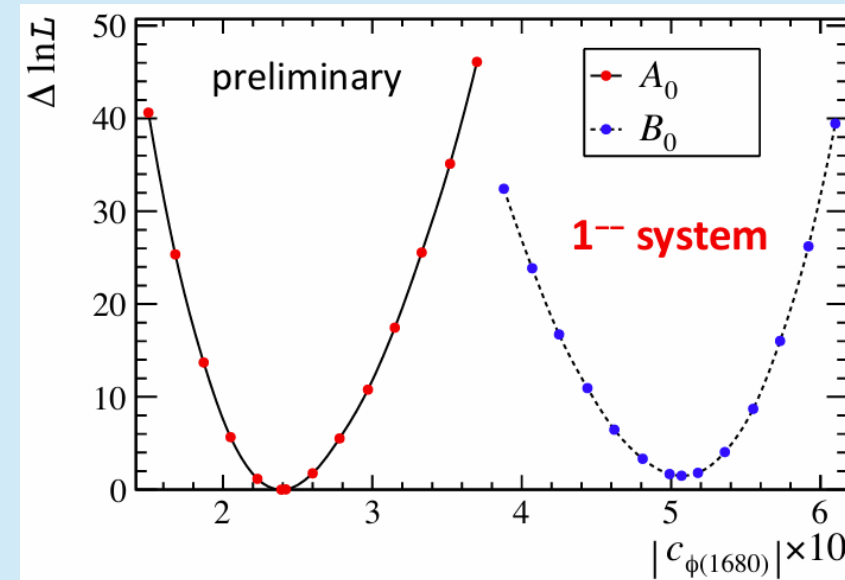
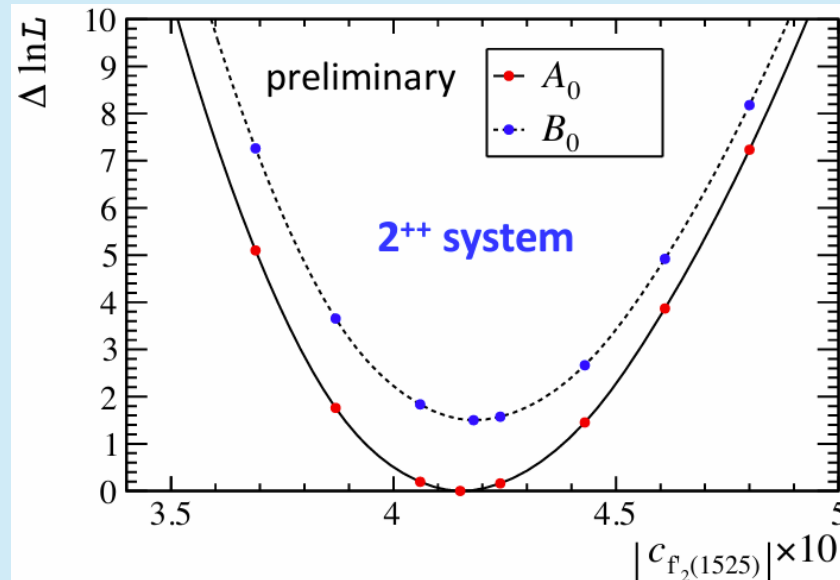
- KK states are well-established with large $\Delta\ln\mathcal{L}$ gain and isobar significance
- Nonresonant state: P-wave (1^{--}), uniformly in mass with constant phase
- Several distinct tensor states give similar significances.

State	J^{PC}	μ_R (MeV/ c^2)	Γ_R (MeV)	\mathcal{B}_{K+K-} (%)	$ c_R $ ($\times 10$)	$(\chi^2_{ c_R })$	$\Delta\ln\mathcal{L}$
$\phi(1020)$	1^{--}	1019.461 ± 0.016	4.249 ± 0.013	49.2 ± 0.5	10 (fix)	-	-
$f'_2(1525)$	2^{++}	1517.4 ± 2.5	86 ± 5	43.8 ± 1.1	4.16 ± 0.09 (2270)	-	-
$\phi(1680)$	1^{--}	1689 ± 12 (*)	211 ± 24 (*)	seen	2.40 ± 0.15 (266)	+304	
$f_2(1270)$	2^{++}	1275.5 ± 0.8	$186.6^{+2.2}_{-2.5}$	$2.30^{+0.25}_{-0.20}$	1.07 ± 0.17 (41)	+18	
$\phi_3(1850)$	3^{--}	1854 ± 7	87^{+28}_{-23}	seen	0.61 ± 0.16 (14)	+15	
$f_2(2010)$	2^{++}	2011^{+62}_{-76}	202^{+67}_{-62}	seen	0.74 ± 0.18 (16)	+13	
$(KK)_{NR}$	1^{--}	-	-	-	0.79 ± 0.26 (10)	+17	

Amplitude analysis of $B_s^0 \rightarrow KK\gamma$

LHCb-paper-2024-002

- Several quasi-degenerate solutions with similar $\Delta \ln L$
 - Weakly constrained interference pattern
 - Preferred solution is with the smallest fit-fractions and constructive interferences of the individual states



Amplitude analysis of $B_s^0 \rightarrow KK\gamma$

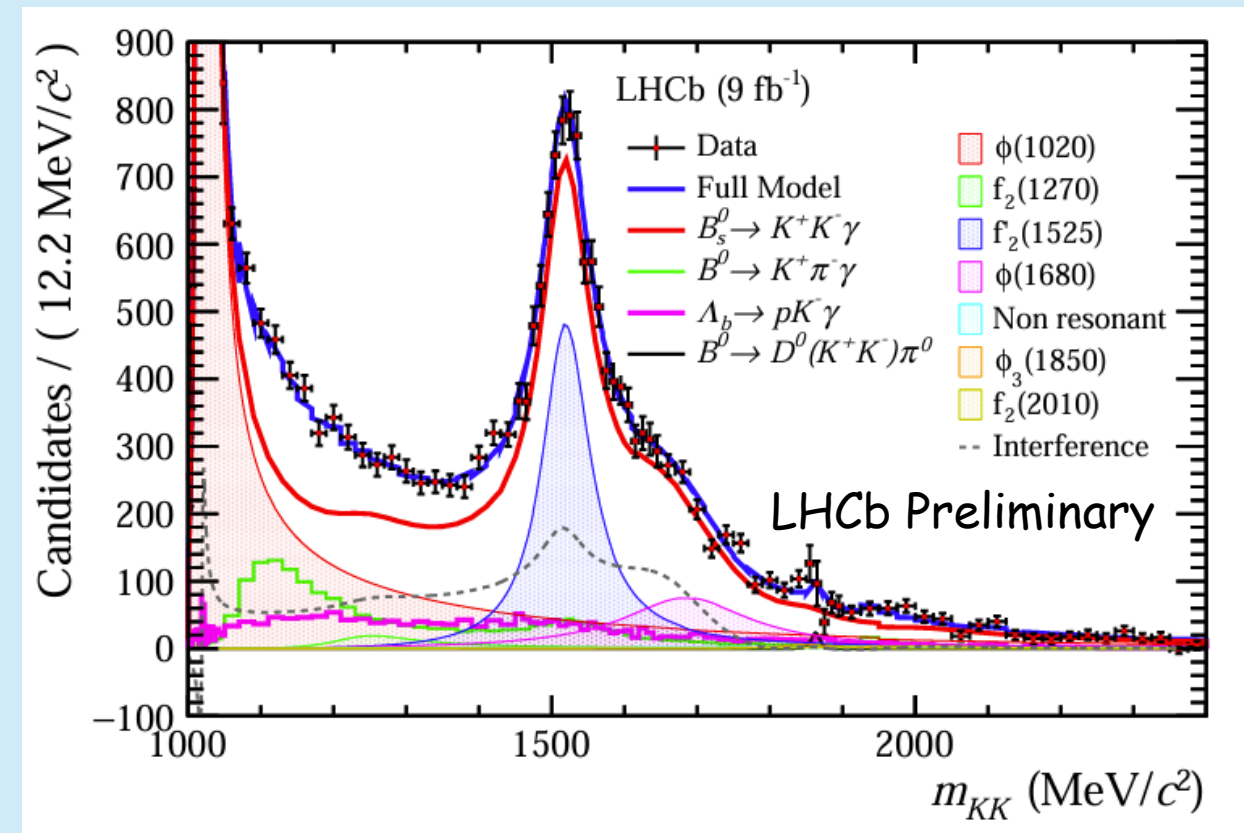
LHCb-paper-2024-002

- Best fit

- Signal yield: $(44.4 \pm 0.5) \times 10^3$
- The overall tensor states (f_2) fit-fraction is $(16.8 \pm 0.5 \pm 0.7)\%$
- A new radiative decay is observed for the first time

$$\frac{\mathcal{B}(B_s^0 \rightarrow f'_2 \gamma)}{\mathcal{B}(B_s^0 \rightarrow \phi \gamma)} = 0.194^{+0.009}_{-0.008} \text{ (stat)}^{+0.014}_{-0.005} \text{ (syst)} \pm 0.005 \text{ (BR)}$$

- Mass and width of $f'_2(1525)$ are measured in good agreement with current world average and measurements



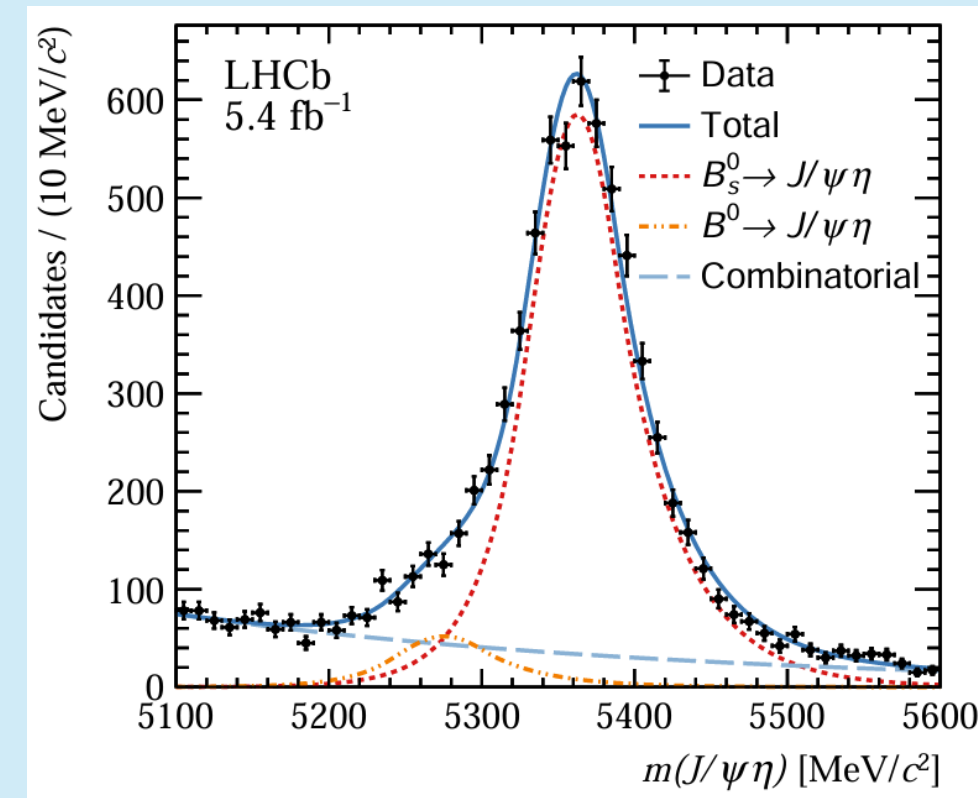
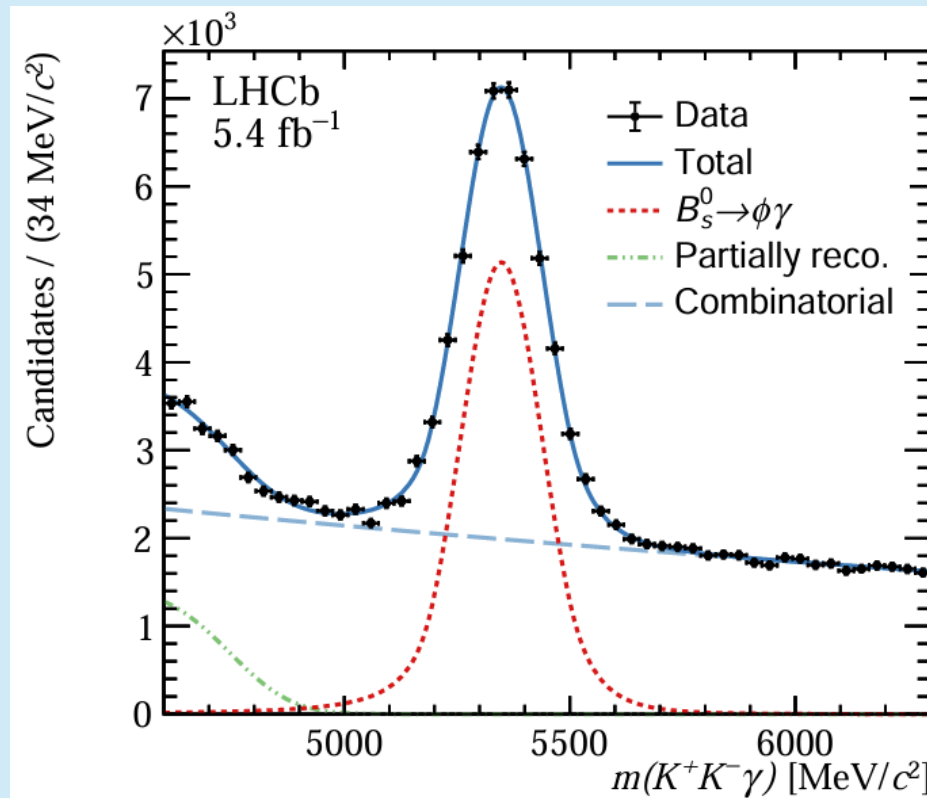
Conclusions

- New results from LHCb
 - First direct search of $B_s \rightarrow \mu^+ \mu^- \gamma$ (**ULs in low q^2 region**)
 - Amplitudes of $\Lambda_b \rightarrow p K^- \gamma$ and $B_s \rightarrow K^+ K^- \gamma$ (**new decay observed!**)
- The precision and sensitivity of the LHCb radiative decay measurements can be improved with Run3 data and results from other experiments
- More results from Run1 and Run2 data are undergoing
 - CPV and branching fraction measurements, amplitude analyses...
- Stay tuned for the coming results!

BACKUP

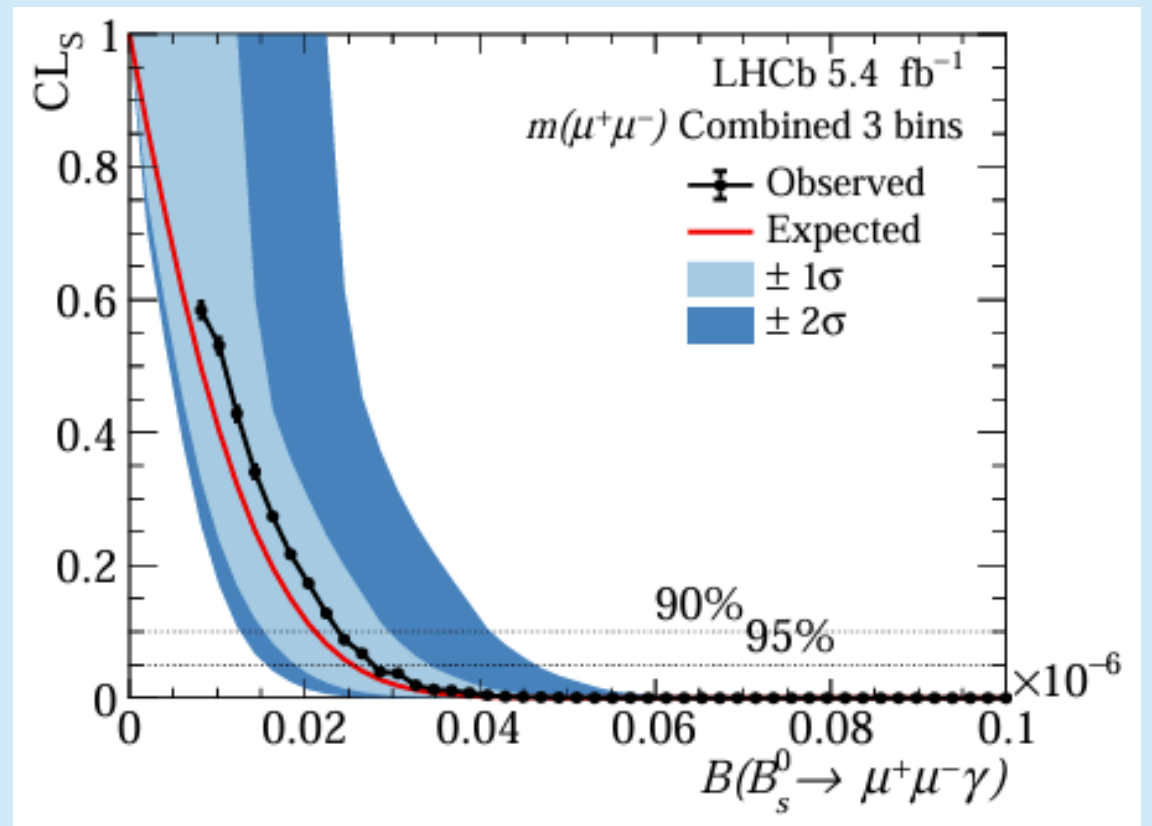
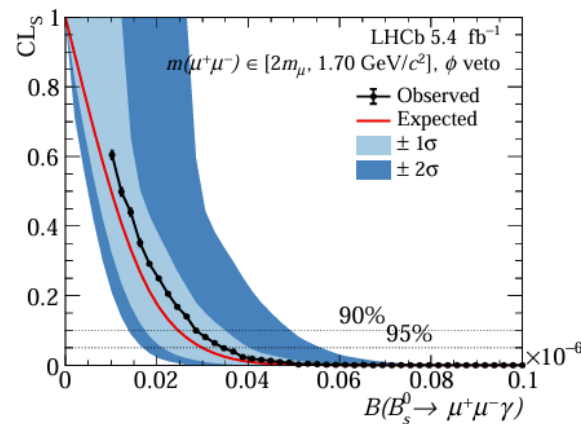
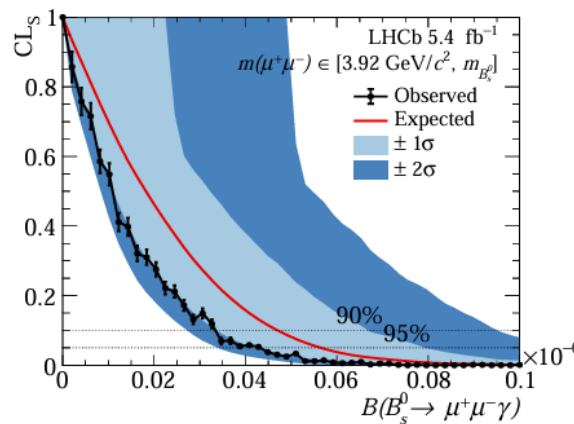
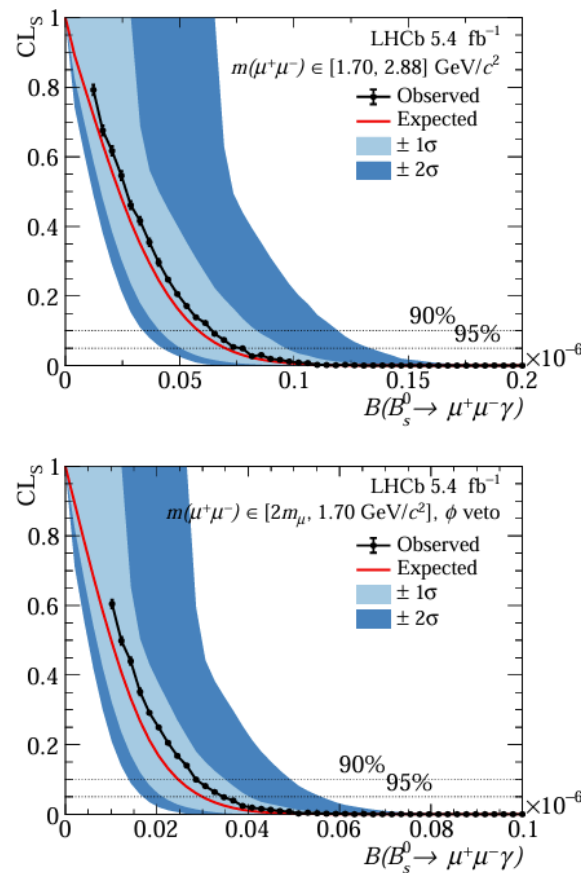
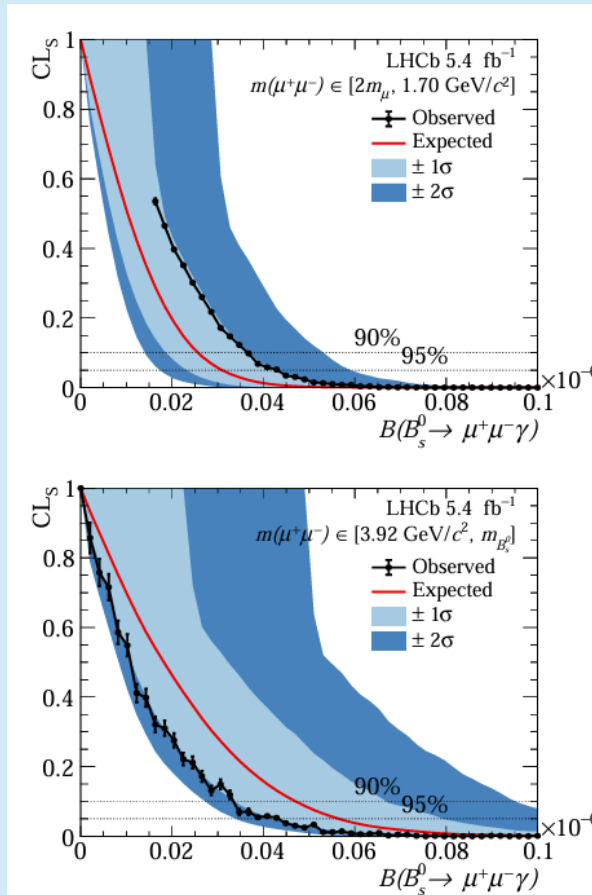
$B_s^0 \rightarrow \mu\mu\gamma$

- Mass fit to the control channel and normalization channel data.

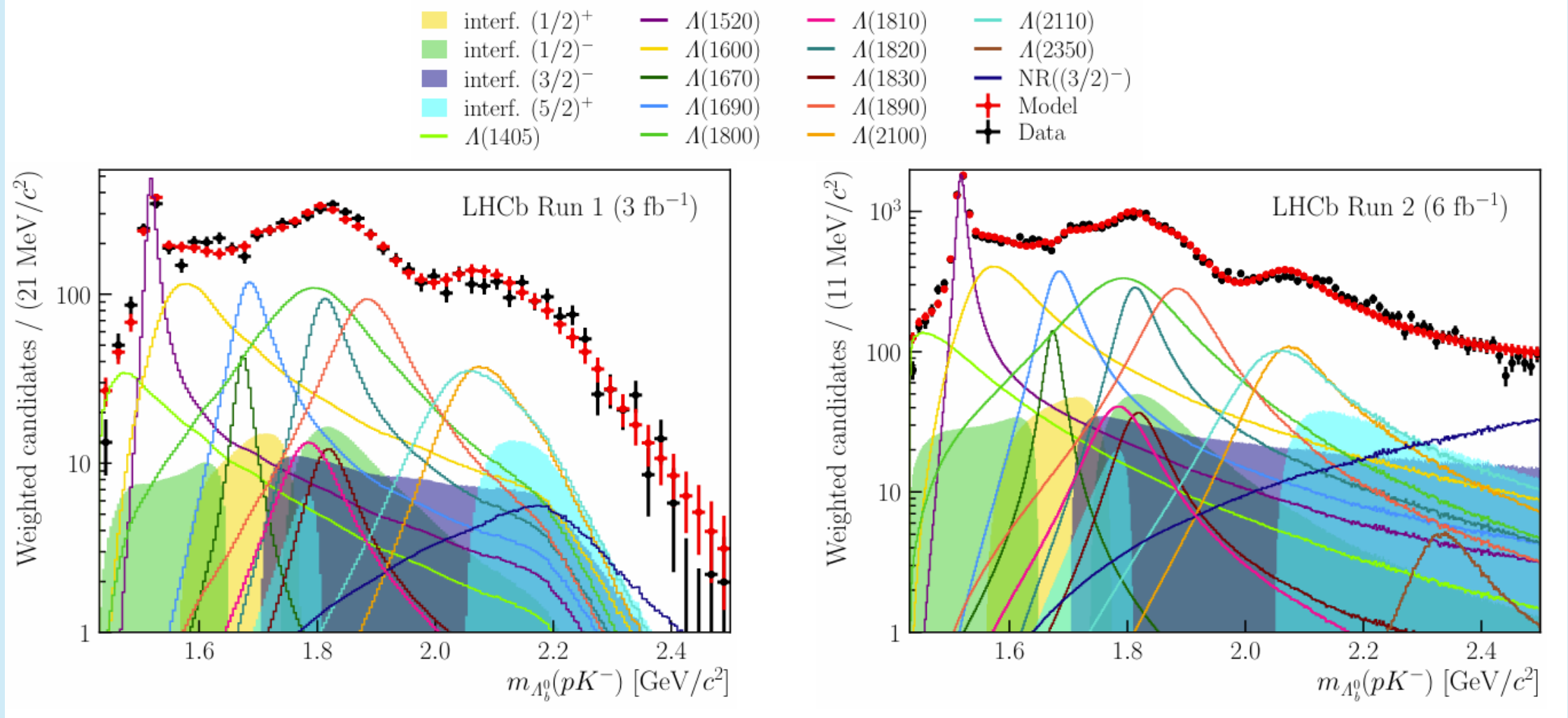


$B_s \rightarrow \mu\mu\gamma$

- CL scans in different q^2 regions



$\Lambda_b \rightarrow p K \gamma$



$\Lambda_b \rightarrow p K \gamma$

- Fit and interference fractions

Observable	Value	σ_{stat}	$\sigma_{\text{syst}}^{\text{internal}}$	$\sigma_{\text{syst}}^{\text{external}}$	σ_{syst}
$\Lambda(1405)$	3.5	+0.3 -0.4	+0.9 -0.0	+1.3 -0.6	+1.9 -0.3
$\Lambda(1520)$	10.4	+0.4 -0.2	+0.7 -0.0	+1.7 -1.6	+2.2 -1.2
$\Lambda(1600)$	15.6	+0.6 -0.9	+0.8 -0.2	+3.9 -5.0	+4.3 -4.6
$\Lambda(1670)$	1.3	+0.2 -0.2	+0.3 -0.2	+1.2 -0.3	+1.3 -0.2
$\Lambda(1690)$	7.7	+0.4 -0.8	+1.8 -0.1	+5.1 -1.0	+6.2 -0.2
$\Lambda(1800)$	18.3	+1.3 -1.6	+1.4 -1.1	+3.2 -6.0	+3.2 -6.2
$\Lambda(1810)$	0.1	+0.9 -0.4	+1.7 -0.4	+4.0 -0.7	+4.8 -0.7
$\Lambda(1820)$	8.3	+0.4 -0.7	-0.2 -1.4	+1.9 -4.8	+1.0 -5.7
$\Lambda(1830)$	0.3	+0.4 -0.4	+0.6 -0.5	+1.5 -0.9	+1.6 -0.9
$\Lambda(1890)$	11.2	+0.7 -0.6	+0.5 -0.6	+4.3 -5.1	+4.6 -4.9
$\Lambda(2100)$	7.3	+0.5 -0.5	+1.1 -0.6	+1.1 -2.8	+1.4 -2.9
$\Lambda(2110)$	6.5	+0.6 -0.7	+1.7 -0.0	+5.4 -0.9	+6.3 -0.2
$\Lambda(2350)$	1.0	+0.2 -0.1	+0.8 -0.0	+0.0 -0.2	+0.8 -0.1
NR($3/2^-$)	2.8	+0.5 -0.4	+0.2 -1.9	+3.0 +0.3	+2.4 -1.3

$\Lambda(1405), \Lambda(1670)$	-0.7	+0.1	+0.2	+0.5	+0.5
$\Lambda(1405), \Lambda(1800)$	7.6	+0.7	+1.2	+0.6	+0.9
$\Lambda(1520), \Lambda(1690)$	0.5	+0.5	+0.3	+0.6	+0.5
$\Lambda(1520), \text{NR}({3/2}^-)$	-0.6	+0.4	+1.0	+1.6	+2.1
$\Lambda(1600), \Lambda(1810)$	-1.9	+1.5	+1.3	+4.1	+3.9
$\Lambda(1670), \Lambda(1800)$	-4.8	+0.5	+0.4	+1.5	+1.5
$\Lambda(1690), \text{NR}({3/2}^-)$	3.9	+0.4	+0.1	+1.2	+0.3
$\Lambda(1820), \Lambda(2110)$	1.1	+0.7	+0.2	+2.5	+1.9